User-Centric Distributed Massive MIMO Systems: Is Scalability Beneficial for Indoor Environments?

Michael A. S. da Costa, Marx M. M. Freitas, Daynara D. Souza,
André M. Cavalcante, Roberto M. Rodrigues, and João C. W. A. Costa

***Abstract*— This work investigates the impacts on the performance of user-centric (UC) distributed massive multiple-input multiple-output (D-mMIMO) networks when following scalability requirements in indoor and outdoor environments. Initially, D-mMIMO systems used the canonical approach, connecting all radio units (RUs) to all user equipment (UEs), but this approach proved impractical. In response, scalable systems emerged, which require limiting the number of UEs that a RU can serve. Therefore, to investigate whether this scalability criterion is equally effective in indoor and outdoor environments, we first propose a strategy that guarantees a minimum number of RUs for each UE. Second, we present an approach that makes this scalability requirement more flexible by increasing the number of UEs that an RU can serve. The simulation results indicate that in an indoor environment, the network presents better spectral efficiency (SE) when more RUs serve the UEs. Also, the proposed method shows an increase in average SE compared to a scalable system and 47% less computational complexity (CC) compared to an unscalable one. Furthermore, flexibilizing the scalability requirement in the indoor environment allowed for the improvement of SE but increased CC. However, in the outdoor environment, for this same approach, there was a decline in SE and an increase in CC.**

***Keywords*— Distributed massive MIMO, indoor and outdoor environments, scalability, spectral efficiency.**

I. Introduction

User-centric (UC) distributed massive multiple-input multiple-output (D-mMIMO), also known as cell-free (CF) mMIMO stands out as one of the technological solutions for future mobile communication networks (6G and beyond) [1], [2]. In these systems, multiple radio units (RUs) are distributed in the coverage area, and each user equipment (UE) is served by a subset of RUs called a cluster of RUs. As a result, UC systems can provide greater macro-diversity and more uniform spectral efficiency (SE) compared to cellular systems [3].

Initially, D-mMIMO systems adopted the approach called canonical cell-free (CCF), where all RUs connect to all UEs, generating a high complexity load with extensive signaling on fronthaul/backhaul links and power consumption, rendering the system unscalable [4], [5]. To address these issues, scalable systems emerge with the requirement to limit the number of UEs per RU. This scalability requirement ensures that the network resources remain finite even as the number of UEs tends to infinity, making the system scalable [3], [4], [6]. However, it is essential to investigate whether following scalability criteria is equally beneficial for indoor and outdoor environments, as several works in the literature claim that meeting scalability requirements results in marginal losses in network SE.

In this regard, this study investigates the effects that adhering to scalability requirements may have on the performance of UC D-mMIMO networks in indoor and outdoor environments. To do so, we employ a method to ensure that a minimum number of RUs serve the UEs of the network, providing an alternative to improving SE for the environments by increasing the number of connections within RU clusters serving UEs. The methodology operates in two ways: one where scalability requirements are not met and another where they are. Additionally, we propose an approach that makes scalability requirements more flexible, allowing each RU to serve more UEs. Analyses are conducted considering different centralized and distributed precoding techniques. Numerical results are presented in terms of SE and computational complexity (CC). The investigation involves varying key parameters, such as the number of UEs that an RU can handle and the minimum number of RUs that can serve a UE, to assess their impact on indoor and outdoor environments. Insightful discussions on the effects of meeting scalability requirements in different environments are conducted.

Notation: Boldface lowercase and uppercase letters denote column vectors and matrices, respectively, the superscript $(\cdot)^{\mathrm{H}}$ denotes the conjugate-transpose operation, the $N \times N$ identity matrix is $\mathbf{I}_N$, and the cardinality of the set $\mathcal{A}$ is represented by $|\mathcal{A}|$. The trace, euclidean norm and expectation operator are denoted as $\mathrm{tr}(\,.\,)$, $\|\,.\,\|$ and $\mathbb{E}\{\,.\,\}$, respectively, and the notation $\mathcal{N}_{\mathbb{C}}\left(\mu, \sigma^2\right)$ stands for a complex Gaussian random variable with mean μ and variance σ^2.

II. System Model

We consider a D-mMIMO system consisting of L RUs, each equipped with N antennas, and K single-antenna UEs. The total number of antennas considering all RUs is $M = NL$. The RUs are connected to a central processing unit (CPU) through fronthaul links that assumed to be error-free and able to support the data traffic. The system operates in time-division duplex (TDD) mode and considers that the uplink (UL) and downlink (DL) channels are reciprocal. The channel vector

Michael A. S. da Costa[1], Marx M. M. Freitas[1], Daynara D. Souza[1], André M. Cavalcante[2], Roberto M. Rodrigues[1], and João C. W. A. Costa[1]. [1]Applied Electromagnetism Laboratory, Federal University of Pará - UFPA, Belém, Brazil, [2]Ericsson Research, Ericsson Telecomunicações Ltda., Indaiatuba, Brazil. E-mails: michael.costa@itec.ufpa.br; marx@ufpa.br; daynara@ufpa.br; andre.mendes.cavalcante@ericsson.com; rmr@ufpa.br; jweyl@ufpa.br. This work was supported by Ericsson Telecomunicações Ltda, ISACI, CNPq and CAPES.

$\mathbf{h}_{kl} \in \mathbb{C}^{N\times 1}$ between the UE k and RU l is modeled as an independent Rician channel, being expressed as [7]

$$\mathbf{h}_{kl} = \underbrace{\sqrt{\frac{\kappa_{kl}}{1+\kappa_{kl}}}\mathbf{h}_{kl}^{\mathrm{LOS}}\, e^{j\theta_{kl}}}_{\overline{\mathbf{h}}_{kl}} + \underbrace{\sqrt{\frac{1}{1+\kappa_{kl}}}\mathbf{h}_{kl}^{\mathrm{NLOS}}}_{\widetilde{\mathbf{h}}_{kl}}, \quad (1)$$

where $\overline{\mathbf{h}}_{kl}$ represents the deterministic line-of-sight (LOS) component and $\widetilde{\mathbf{h}}_{kl}$ denotes the non-line-of-sight (NLOS) component. The term $\theta_{kl} \sim \mathcal{U}[0, 2\pi)$ stands for random phase shifts that may occur in the LOS component due to UE's mobility. The Rician factor κ_{kl} denotes the power ratio between the LOS and NLOS components, defined as $\kappa_{kl} = p_{\mathrm{LOS}}/(1-p_{\mathrm{LOS}})$, where p_{LOS} represents the probability of the LOS component existing, being zero for propagation links that are exclusively NLOS. The LOS component between RU l and UE k can be expressed as

$$\mathbf{h}_{kl}^{\mathrm{LOS}} = \sqrt{\beta_{kl}}\left[1, \cdots, e^{\mathrm{j}(N-1)\pi \sin(\varphi_{kl})\cos(\phi_{kl})}\right]^{\mathrm{T}}, \quad (2)$$

where the azimuth angle is represented by φ_{kl}, ϕ_{kl} means the elevation angle, and the large-scale fading gain, which includes path loss and shadowing, is denoted by β_{kl}. The NLOS propagation undergoes a correlated Rayleigh fading, being expressed as

$$\mathbf{h}_{kl}^{\mathrm{NLOS}} = \sqrt{\mathbf{R}_{kl}^{\mathrm{NLOS}}}\,\mathbf{g}_{kl}, \quad (3)$$

where the vector $\mathbf{g}_{kl} \in \mathbb{C}^{N\times 1}$ is formed by elements that are independent and identically distributed (i.i.d.) Gaussian $\mathcal{N}_{\mathbb{C}}(0,1)$ random variables (RVs). The correlation matrix $\mathbf{R}_{kl}^{\mathrm{NLOS}}$ is calculated according to the Gaussian spatial correlation model of local scattering presented in [6]. Then, leading to $\widetilde{\mathbf{R}}_{kl} = \mathbb{E}\{\tilde{\mathbf{h}}_{kl}\tilde{\mathbf{h}}_{kl}^{\mathrm{H}}\} = \mathbf{R}_{kl}^{\mathrm{NLOS}}/(\kappa_{kl}+1)$.

A. Uplink Training

Each coherence block comprises τ_c complex-valued samples, where τ_p samples are dedicated for UL pilot signals, and τ_d samples are reserved for DL data transmissions. During the training phase, the UEs transmit pilot signals to the RUs to estimate their communication channels. These pilot signals of length τ_p are designed to be orthogonal to each other, and some UEs can reuse a pilot t_k if $K > \tau_p$. Let $\mathcal{P}_k \subset \{1,\ldots,K\}$ denote the subset of UEs assigned to the pilot t_k. The received pilot signal at RU l is given by [6]

$$\mathbf{y}_{t_k l}^{\mathrm{pilot}} = \sum_{i\in\mathcal{P}_k} \sqrt{\tau_p \eta_i}\,\mathbf{h}_{il} + \mathbf{n}_{t_k l}, \quad (4)$$

where $\mathbf{n}_{t_k l} \sim \mathcal{N}_{\mathbb{C}}\left(\mathbf{0_N}, \sigma_{ul}^2 \mathbf{I}_N\right)$ denotes the noise and η_i corresponds to the power transmitted by UE i in the UL direction. The channel estimation using the linear minimum mean square error (LMMSE) can be computed as

$$\widehat{\mathbf{h}}_{kl} = \sqrt{\tau_p \eta_k}\mathbf{R}_{kl}\boldsymbol{\Psi}_{t_k l}^{-1}\mathbf{y}_{t_k l}^{\mathrm{pilot}}, \quad (5)$$

where $\mathbf{R}_{kl} = \mathbb{E}\{\mathbf{h}_{kl}\mathbf{h}_{kl}^{\mathrm{H}}\} = (\overline{\mathbf{h}}_{kl}\overline{\mathbf{h}}_{kl}^{\mathrm{H}} + \widetilde{\mathbf{R}}_{kl})$ e $\boldsymbol{\Psi}_{t_k l} = \mathbb{E}\{(\mathbf{y}_{t_k l}^{\mathrm{pilot}})(\mathbf{y}_{t_k l}^{\mathrm{pilot}})^{\mathrm{H}}\} = \sum_{i\in\mathcal{P}_k}\eta_i\tau_p(\overline{\mathbf{h}}_{il}\overline{\mathbf{h}}_{il}^{\mathrm{H}} + \widetilde{\mathbf{R}}_{il}) + \sigma_{\mathrm{ul}}^2\mathbf{I}_N$.

B. Downlink Data Transmission

In UC systems, each UE is associated with a subset of RUs called an RU cluster, represented by $\mathcal{M}_k \subset \{1,\ldots,L\}$. The connections between UE k and the RU are represented by a diagonal matrix $\mathbf{D}_{kl} \in \mathbb{N}^{N\times N}$, defined as

$$\mathbf{D}_{kl} = \begin{cases} \mathbf{I}_N & \text{if } l \in \mathcal{M}_k \\ \mathbf{0}_N & \text{if } l \notin \mathcal{M}_k. \end{cases} \quad (6)$$

The set of UEs served by an RU is indicated by $\mathcal{D}_l$, and are limited to $|\mathcal{D}_l| \le U_{max}$ to ensure system scalability [3]. The symbol intended for UE k is represented by $s_k \in \mathbb{C}$. The received signal at UE k can be described as

$$y_k^{dl} = \sum_{l=1}^{L}\underbrace{\mathbf{h}_{kl}^{\mathrm{H}}\mathbf{D}_{kl}\mathbf{w}_{kl}s_k}_{\text{Desired signal}} + \sum_{i=1,i\neq k}^{K}\sum_{l=1}^{L}\underbrace{\mathbf{h}_{kl}^{\mathrm{H}}\mathbf{D}_{il}\mathbf{w}_{il}s_i}_{\text{Interfering signals}} + \underbrace{n_k}_{\text{Noise}}, \quad (7)$$

where $\mathbf{x}_l = \sum_{k=1}^{K}\mathbf{D}_{kl}\mathbf{w}_{kl}s_k$ represents the data signal sent by RU l, $\mathbf{w}_{kl}$ denotes the precoding vector, and $n_k \sim \mathcal{N}_{\mathbb{C}}\big(0, \sigma_{\mathrm{dl}}^2\big)$ is the received noise. The terms s_k e $\mathbf{w}_{kl}$ satisfy $\mathbb{E}\{\|s_k\|^2\} = 1$ and $\mathbb{E}\{\|\mathbf{w}_{kl}\|^2\} = \rho_{kl}$, with ρ_{kl} being the power allocated to UE k relative to RU l.

C. Spectral Efficiency

The SE is a metric that quantifies the amount of data transmitted in a wireless communication system relative to the time and bandwidth available. The SE is expressed in bits/s/Hz and an achievable DL SE can be computed as [3]

$$\mathrm{SE}_k = \frac{\tau_c - \tau_p}{\tau_c}\log_2\left(1+\mathrm{SINR}_k\right), \quad (8)$$

where $(\tau_c - \tau_p)/\tau_c$ represents the pre-log factor, which is the fraction of samples per coherence block used to transmit the DL data. The term SINR_k is the signal-to-interference-plus-noise ratio (SINR), which can be given by

$$\mathrm{SINR}_k = \frac{\left|\mathbb{E}\left\{\mathbf{h}_k^{\mathrm{H}}\mathbf{D}_k\mathbf{w}_k\right\}\right|^2}{\sum_{i=1}^{K}\mathbb{E}\left\{\left|\mathbf{h}_k^{\mathrm{H}}\mathbf{D}_i\mathbf{w}_i\right|^2\right\} - \left|\mathbb{E}\left\{\mathbf{h}_k^{\mathrm{H}}\mathbf{D}_k\mathbf{w}_k\right\}\right|^2 + \sigma_{\mathrm{dl}}^2}, \quad (9)$$

where $\mathbf{w}_k \in \mathbb{C}^{M\times 1}$ and $\mathbf{h}_k \in \mathbb{C}^{M\times 1}$ are, respectively, the collective vectors of $\mathbf{w}_{kl}$ and $\mathbf{h}_{kl}$. For instance, $\mathbf{w}_k = \left[\mathbf{w}_{k1}^{\mathrm{T}}, ..., \mathbf{w}_{kL}^{\mathrm{T}}\right]^{\mathrm{T}}$ for $l \in \{1,\cdots,L\}$. Moreover, $\mathbf{D}_k = \mathrm{diag}\left(\mathbf{D}_{k1}, ..., \mathbf{D}_{kL}\right) \in \mathbb{N}^{M\times M}$ stands for the diagonal block matrix. Note that (8) represents the widely known hardening bound, which is a capacity lower bound valid for any choice of precoding vectors [3].

III. RU CLUSTER EXPANSION METHOD TO CONTROL MINIMUM NUMBER OF RUS PER UE

This work proposes a strategy to ensure that each UE in the network is connected to a minimum number of RUs, denoted as C_{min}, $\forall K \in \{1,\ldots,K\}$. The value of C_{min} is defined as $1 \le C_{\mathrm{min}} \le L$. This strategy is designed to operate in two ways: either not following the scalability requirement or following it. The goal in both cases is to increase the cardinality $|\mathcal{M}_k|$ of the RU clusters to enhance

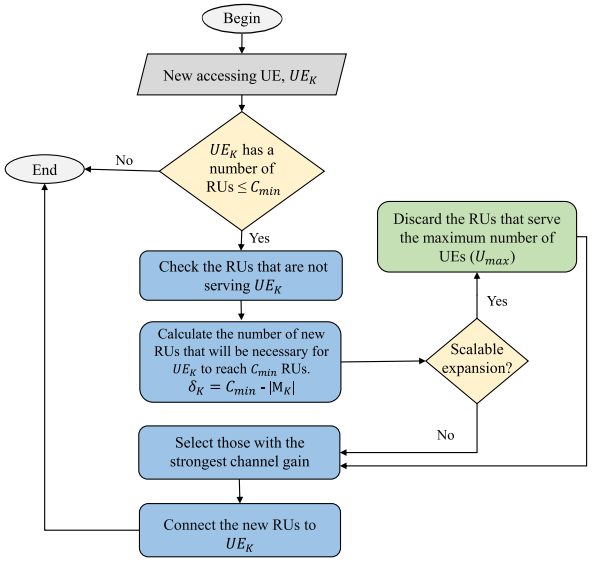

Fig. 1: Flowchart of the proposed approach to ensure that users associate with a minimum number of RUs, denoted as C_{min}.

SE. The flowchart shown in Fig. 1 provides an overview of the operation of C_{min}.

For the first case, when the scalability requirement is not respected, as soon as a cluster of RU, denoted by $|\mathcal{M}_k|$, is created for the UE, the CPU checks if $|\mathcal{M}_k|$ is under the condition of $|\mathcal{M}_k| < C_{\text{min}}$. If true, the CPU is activated to connect the RUs with the strongest channel gain to make $|\mathcal{M}_k| = C_{\text{min}}$. For this purpose, the subset $\mathcal{E}_k$ is created, containing the indices of the RUs that do not serve the UE, organized according to the strongest channel gain, $\beta_{k1} \geq \beta_{k2} \geq \ldots \geq \beta_{kl}$, where β_{kl} denotes the large-scale fading of the k-th UE to the l-th RU. Then, the CPU calculates $\delta_k = C_{\text{min}} - |\mathcal{M}_k|$, where δ_k is the number of RUs needed for the UE to reach C_{min}. The CPU then performs the action $\mathbf{D}_{kl} = \mathbf{I}_N$ on the first δ_k indices of the subset $\mathcal{E}_k$.

For the second case, the algorithm follows the same logic described previously until the calculation of the required RUs, δ_k. Next, it checks if scalable expansion has been requested. If so, the indices of the RUs in $\mathcal{E}_k$ that are serving the maximum number of UEs, $|\mathcal{D}_l| = U_{max}$, are discarded. After this step, for the remaining RU indices in $\mathcal{E}_k$, the CPU selects the δ_k RUs with the highest channel gain to serve the UE. From here on, the method described first will be referred to with the prefix "N + the abbreviation of the RU cluster scheme + C_{min}", and the second by the "abbreviation of the RU cluster scheme + C_{min}".

IV. Numerical Results

We consider a D-mMIMO network composed of $K = 20$ UEs and L RUs with N antennas. The UEs are uniformly distributed in a square area, and the RUs follow the hard core point process (HCPP) arrangement. The propagation models and line-of-sight (LOS) probabilities adopted are according to 3GPP TR 38.901 [8], using the Indoor Hotspot Open Office (InH-open) model and Urban Micro (UMi) for indoor and outdoor environments respectively. The simulations focus on DL channels with a carrier frequency of 3.5 GHz and a bandwidth of 100 MHz. The noise figure is 8 dB, and the UL power is 22 dBm per UE in both environments. Additional parameters include antenna spacing of 1/2 wavelength and a shadow fading standard deviation of 4 dB. Other important parameters are listed in Table I. Monte Carlo simulations were performed for various RU/UE locations and different channel realizations. The wraparound technique was used to balance the interference at each RU. The RU clustering schemes from [4], [3], and [9] are referred to as CCF, scalable cell-free (SCF), and matched decision (MD), respectively. The local partial MMSE (LP-MMSE) precoding for the distributed implementation and partial MMSE (P-MMSE) for the centralized implementation were chosen due to their better performance [6], [10]. The CC is calculated as in [6], accounting for the sum of the number of complex multiplications required from the network for a generic UE to perform channel estimation and generate the combining vectors in each coherence block.

TABLE I: Parameters for DL simulation.

PARAMETER	INDOOR	OUTDOOR
Number of RUs	20	100
Number of antennas	4	1
Coherence block samples	3750	200
RU and UE heights	3 m, 1.65 m	11.65 m, 1.65 m
RU total Tx power	15 dBm	23 dBm
Coverage area	100m × 100m	1km × 1km

In Fig. 2, we compare the performance of SE using scalable RU clusters, SCF, and non-scalable clusters, CCF, in outdoor and indoor environments.

In Fig. 2a, in the outdoor environment, the cumulative distribution function (CDF) shows that the SE of SCF outperformed that of CCF. This is because the channel gains are weak due to the dimensions of the space, and allowing all RUs to serve all UEs leads to reduced allocated power and increased network interference. Therefore, creating RU clusters is an effective strategy to increase SE in outdoor environments.

On the other hand, in Fig. 2b, a different behavior was observed in the indoor environment: CCF showed better SE performance compared to SCF. Specifically, for the 95% likelihood, P-MMSE increased SE by 1.5 bits, and LP-MMSE by approximately 55%. This is due to the stronger channel gains in this environment, resulting from the reduced dimensions of the space. Therefore, connecting more RUs to the UEs proved to be an effective strategy for increasing SE in indoor environments.

In Fig. 3 and Fig. 4, the performance of the C_{min} method in the indoor and outdoor environments, respectively, are shown, comparing the average SE and CC of the RU clusters. In Fig. 3a, we observe that for both precodings, SCF + C_{min} shows marginal improvements in SE compared to SCF. This occurs because when the RU clusters are created, most of the RUs are already being used at maximum capacity $|\mathcal{D}_l| = U_{max}$. On the other hand, NSCF + C_{min} in LP-MMSE shows SE equal to CCF at C_{min} = 12 and reaches its maximum value at C_{min} = 14; beyond this value, the precoding cannot handle the interference and converges to SE values close to CCF.

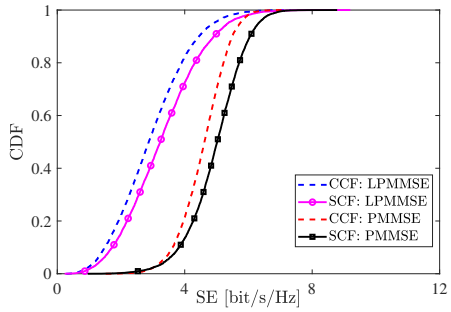

(a) Outdoor environment. Parameters setting: $L = 100$, $N = 1$ e $K = 20$.

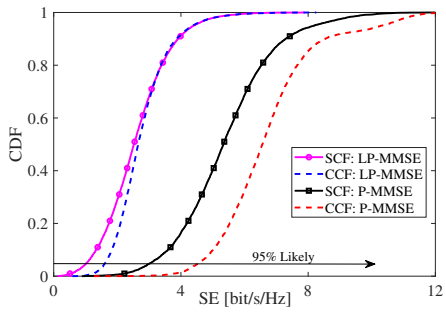

(b) Indoor environment. Parameters setting: $L = 20$, $N = 4$ e $K = 20$.

Fig. 2: Comparison of the SE in outdoor and indoor environments under $U_{max} = 10$.

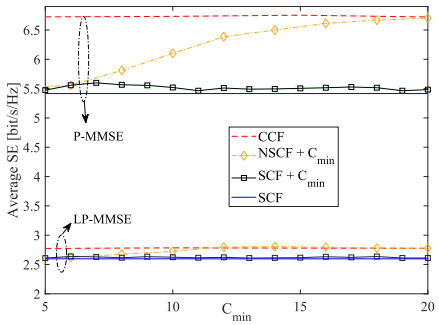

(a) Average DL SE versus C_{min}.

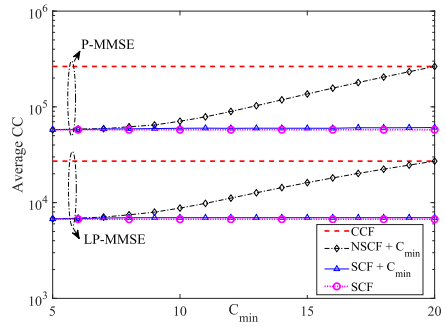

(b) Average CC versus C_{min}.

Fig. 3: Average DL SE and CC achieved by varying C_{min} in indoor environment. Parameters settings: $U_{max} = 10$, $K = 20$, $L = 20$, $N = 4$.

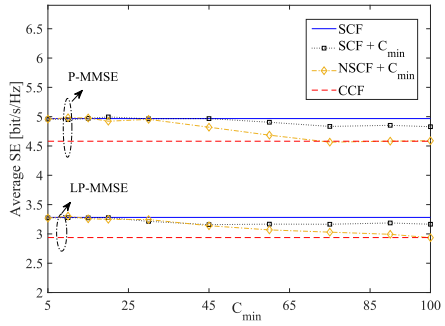

(a) Average DL SE versus C_{min}

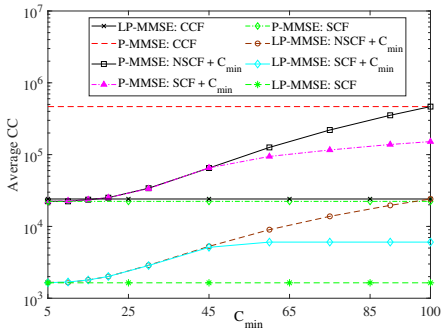

(b) Average CC versus C_{min}.

Fig. 4: Average DL SE and CC achieved by varying C_{min} in outdoor environment. Parameters settings: $U_{max} = 10$, $K = 20$, $L = 100$, $N = 1$.

For P-MMSE, NSCF + C_{min} shows higher SE as C_{min} values increase. This is allowed by the fact that P-MMSE can reduce interference better than LP-MMSE.

In Fig. 3b, a constant increase in the average CC can be observed as C_{min} increases. This makes sense since more UEs are connected to more RUs, and therefore, more channel estimation and combining vectors are required in the network system. However, for the controlled environment, we are considering when the LP-MMSE of NSCF + C_{min} reaches its maximum average SE value, it shows a 47% lower CC than that of CCF. While for P-MMSE, the cost of having higher SE would require higher CC values.

In Fig. 4a, a typical behavior was observed for both precodings in SCF + C_{min} and NSCF + C_{min}. The SE starts overlapping with SCF, but as C_{min} increases, the SE declines due to the increased interference generated by the larger RU clusters. Conversely, in Fig. 4b, as C_{min} increases, the CC also grows. Therefore, increasing the number of RUs per UE in the outdoor scenario can degrade the SE and increase the network CC.

In Fig. 5, the achievable average SE per UE and CC are presented as functions of the maximum number of UEs each RU can serve (U_{max}), varying U_{max} from 5 to 20. We did not subject the SCF to this evaluation since it is naturally limited to τ_p = U_{max} = 10. Instead, we used the scalable RU cluster matched decision (MD) from [9].

In Fig. 5a, it can be observed that, for LP-MMSE, up to U_{max}

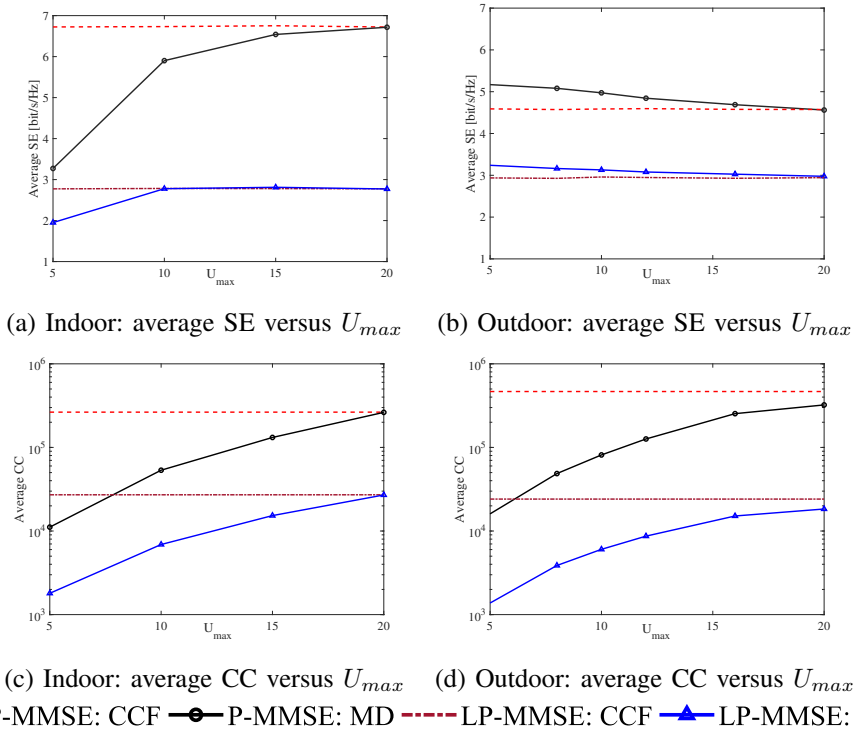

(a) Indoor: average SE versus U_{max} (b) Outdoor: average SE versus U_{max}

(c) Indoor: average CC versus U_{max} (d) Outdoor: average CC versus U_{max}

Fig. 5: Comparison of DL SE and CC under different scalability limits for indoor and outdoor environments. Parameters setting for outdoor: $L = 100$, $K = 20$, $N = 1$. For indoor: $L = 20$, $K = 20$, $N = 4$.

= 10, the additional interference generated by the final cluster of RUs is easily reduced. However, for values greater than this, the interference increases, and the SE stabilizes. On the other hand, P-MMSE manages to mitigate the interference as U_{max} increases, reaching higher SE values. However, we can note that in Fig. 5c, the cost of having a higher SE for P-MMSE is a higher CC in the system. Whereas for LP-MMSE, its maximum SE at U_{max} = 10 shows a 74.5% lower CC when compared to CCF. Conversely, in Fig. 5b, the increase in U_{max} in the outdoor environment becomes detrimental to the network's performance because the precodings cannot reduce the added interference caused by the expansion of RU clusters, and the allocated power is reduced for each UE, in addition to the CC increasing, as shown in Fig. 5d, leading to network losses.

V. Conclusions

This paper investigated the impacts of scalability requirements in outdoor and indoor environments in UC D-mMIMO systems. A method was proposed to control the minimum number of RUs serving the UEs and an approach that flexibilize the scalability requirement by increasing the number of UEs that RUs can serve. The results show that in the indoor environment, SE increases when the scalability criterion is not followed. In particular, LP-MMSE achieves maximum SE with 47% lower CC compared to CCF. When applying flexibility in scalability requirements, indoor SE increases, and so does CC. However, in particular, LP-MMSE achieves maximum SE with 47% lower CC compared to CCF. In the outdoor environment, there was a degradation in SE and an increase in CC when using the proposed approaches. It is concluded that applying the same scalability requirements in indoor and outdoor environments results in different performances. Therefore, it is essential to adapt cluster selection strategies for each specific environment. Prioritizing scalability is advantageous in outdoor environments. In indoor, strategies that expand the size of RU clusters can enhance SE but will also raise CC.

References

[1] I. F. Akyildiz *et al.*, "6G and beyond: The future of wireless communications systems," *IEEE Access*, vol. 8, pp. 133 995–134 030, Jul. 2020.

[2] J. Zhang, S. Chen, Y. Lin, J. Zheng, B. Ai, and L. Hanzo, "Cell-free massive MIMO: A new next-generation paradigm," *IEEE Access*, vol. 7, pp. 99 878–99 888, Jul. 2019.

[3] E. Björnson and L. Sanguinetti, "Scalable cell-free massive MIMO systems," *IEEE Trans. Commun.*, vol. 68, no. 7, pp. 4247–4261, Jul. 2020.

[4] G. Interdonato, P. Frenger, and E. G. Larsson, "Scalability aspects of cell-free massive MIMO," in *Proc. IEEE Int. Conf. Commun. (ICC)*, Jul. 2019, pp. 1–6.

[5] S. Buzzi and C. D'Andrea, "Cell-free massive MIMO: User-centric approach," *IEEE Wireless Commun. Lett.*, vol. 6, no. 6, pp. 706–709, Dec. 2017.

[6] Ö. Demir, E. Björnson, and L. Sanguinetti, *Foundations of User-Centric Cell-Free Massive MIMO*. Foundations and Trends in Signal Processing Series, Now Publishers, 2021.

[7] O. Özdogan, E. Björnson, and E. G. Larsson, "Massive MIMO with spatially correlated Rician fading channels," *IEEE Trans. Commun.*, vol. 67, no. 5, pp. 3234–3250, May 2019.

[8] 3GPP, "5G; Study on channel model for frequencies from 0.5 to 100 GHz," *3rd Generation Partnership Project (3GPP), Technical Report (TR) 38.901 Version 16.1.0 Release 16*, Nov. 2020.

[9] M. Freitas, D. Souza, G. Borges, A. M. Cavalcante, D. B. da Costa, M. Marquezini, I. Almeida, R. Rodrigues, and J. C. W. A. Costa, "Matched-decision AP selection for user-centric cell-free massive MIMO networks," *IEEE Trans. Veh. Technol*, pp. 1–16, Jan. 2023.

[10] E. Björnson and L. Sanguinetti, "Making cell-free massive MIMO competitive with MMSE processing and centralized implementation," *IEEE Trans. Wireless Commun.*, vol. 19, no. 1, pp. 77–90, Jan. 2019.